A Comparative Study of Distance Measures for 2DPCA-Based Face Recognition

Received: 29/07/2025
Revised: 04/08/2025
Accepted: 05/08/2025

W. H. Al-Arashi (1,*)

[1] Faculty of Engineering and Computing, Mechatronics Engineering Department, University of Science and Technology, Aden, Yemen
*Corresponding Author's Email: w.alarashi@ust.edu

A Comparative Study of Distance Measures for 2DPCA-Based Face Recognition

Waled Hussein Al-Arashi
Faculty of Engineering and Computing,
Mechatronics Engineering Department,
University of Science and Technology,
Aden, Yemen
w.alarashi@ust.edu

Abstract— Face recognition is considered a primary technology in biometric systems. Despite its merits, the systems suffer because of the various facial variations. Two-Dimensional Principal Component Analysis (2DPCA) limits these variations by preserving facial spatial information and, at the same time, improves the computational efficiency. Those features give it an advantage in different applications, not only in face recognition but also in artificial intelligence (AI) applications. However, the distance methods used for classifications associated with 2DPCA are a significant issue. This paper explores and modifies various distance measures defined in the literature of the PCA approach for face recognition. These fourteen-distance metrics are modified and compared to the standard Euclidean distance on well-known face databases, namely the ORL, AR, and LFW databases. The experiments on these databases, which have diverse variations in facial images, manifest the superiority of the correlation coefficient-based distance method. Additionally, the results also show remarkable performance of angle-based and Canberra distance methods. These results clarify the importance of this work in enhancing distance metrics within 2DPCA algorithms to enhance the accuracy and robustness of both traditional and AI-driven recognition systems.

Keywords—Two-dimensional PCA, Face recognition, Classification Methods.

I. INTRODUCTION

Face recognition has become a cornerstone of modern biometric systems. This is primarily because of its natural, non-intrusive, and easily deployable attributes in a variety of real-world contexts—from security and surveillance to access control and human-computer interaction [1]. Nevertheless, despite these strengths, achieving high levels of accuracy poses significant challenges due to substantial variations in facial appearance arising from illumination, expression, aging, pose, occlusion, and image quality [1], [23].

Face recognition algorithms are divided into three groups: appearance-based methods, feature-based methods, and hybrid methods. Appearance-based approaches examine holistic pixel intensity data and encompass famous and well-known techniques such as Principal Component Analysis (PCA), Linear Discriminant Analysis (LDA), and Independent Component Analysis (ICA) [2-7]. Feature-based methods focus on extracting local or geometric face characteristics, such as facial landmarks, whereas hybrid methods merge both global and local approaches to enhance robustness.

Among these various techniques, PCA has been widely adopted due to its effectiveness in minimizing dimensionality while preserving essential key variability in facial data [3-4]. PCA transforms high-dimensional face images into a compact set of uncorrelated features, referred to as principal components, which can be utilized for efficient classification. Nevertheless, PCA requires vectorizing two-dimensional images, which leads to the loss of crucial spatial information, potentially impairing recognition performance [8-10].

Following the PCA projection, selecting an appropriate distance measure for comparing feature vectors plays a crucial role in recognition performance. The Euclidean distance is the most frequently employed metric due to its simplicity; nevertheless, other distances, such as Mahalanobis, cosine-based, and correlation-based distances, have proven to offer greater accuracy concerning PCA-based systems [13, 20].

To mitigate the loss of spatial information, Two-Dimensional PCA (2DPCA) is introduced, operating directly on image matrices without the requirement for vectorization [9]. 2DPCA effectively preserves spatial structure and offers superior computational efficiency compared with PCA [9, 10]. Extensions and variants of 2DPCA, including Diagonal PCA (DiaPCA) [10], Selected Coefficient 2DPCA [11], Variation 2DPCA [12], Relaxed 2DPCA [21], and Joint-norm 2DPCA [22], have been developed to further improve both discrimination and robustness.

Recently, the integration of 2DPCA and its variants into artificial intelligence (AI) pipelines has gained significant interest [21-33]. Shallow subspace representations, such as 2DPCA, are frequently utilized as feature extraction stages before feeding data into deep learning models, facilitating hybrid systems that combine traditional statistical methods and neural networks [26, 27]. The implementation of effective distance measures in these intermediate stages can enhance performance in various tasks such as identity verification, clustering, and few-shot learning [28]. Furthermore, they play a critical role in privacy-preserving face systems [29]. Beyond the realm of face recognition, 2DPCA has also been employed as an effective shallow feature extraction technique in AI-driven applications, such as texture classification [26], where it contributes to the enhancement of convolutional neural networks (CNNs) performance when combined in hybrid architectures [30]. In medical image analysis, 2DPCA has also been used to enhance feature representations before feeding them into deep classifiers for tasks such as disease diagnosis and lesion detection [27, 31]. For hyperspectral image classification, 2DPCA aids in dimensionality reduction while preserving spatial-spectral information, yielding better results when integrated with deep learning frameworks [28, 32]. Likewise, in handwriting recognition, 2DPCA-based features have been combined with deep neural networks to improve accuracy in multilingual character recognition systems [29, 33]. As AI-driven recognition systems continue to evolve, understanding and optimizing these distance measures within 2DPCA frameworks has become increasingly crucial for developing robust, efficient, and interpretable solutions.

Thus, studying and optimizing distance measures in 2DPCA-based algorithms is essential not only for enhancing traditional face recognition accuracy but also for advancing AI applications that depend on robust similarity measurement [21-22, 24-25]. In systems powered by AI, feature extraction techniques such as 2DPCA often serve as a bridge between raw data and deep learning classifiers or embedding models [26-27], 30-31]. The choice of distance metric has a direct impact on subsequent tasks such as clustering, identity verification, few-shot learning, and adversarial robustness [28, 32]. By enhancing the discriminative power of 2DPCA feature spaces with optimized distance functions, these systems can achieve higher generalization ability and stability across diverse datasets and operational conditions [22, 25, 33]. Furthermore, these enhancements can lead to more interpretable and trustworthy AI models, which is particularly crucial for applications involving security, healthcare, and human-centered AI solutions [31-32, 34]. As a result, systematically investigating distance measures within the 2DPCA framework offers a foundation for building more powerful and reliable hybrid AI systems [21, 25, 30, 34].

In spite of advancements in feature extraction, most 2DPCA-based face recognition systems continue to rely primarily on Euclidean distance for classification. Nevertheless, 2DPCA-based studies have shown that alternative distance measures, including volume-based, assembled matrix, reweighted angle, RowAMD, and row-kNN distances, can lead to significant improvements [16–20, 35-36]. Applying these advanced distance measures within the 2DPCA framework remains an open question for further research.

Motivated by this gap, this paper explores fourteen distance measures, originally developed for PCA-based recognition, and modifies them to 2DPCA-based systems. The evaluation of their impact on recognition accuracy is conducted using standard face datasets under various conditions, including changes in illumination and expression.

The remaining of this paper is organized as follows. Section 2 briefly explains a 2DPCA algorithm. Section 3 depicts modified versions of the distance measures. Section 4 provides experimental results and discussion on three famous face databases. Finally, section 5 introduces the conclusion and future work.

II. 2DPCA ALGORITHM

Let us consider a random matrix A characterized by dimensions $m \times n$, which projects onto an X n-dimensional unitary column vector via linear transformation as illustrated in Eq. (1):

$$\boldsymbol{Y} = \boldsymbol{AX} \tag{1}$$

Y is referred to as the projected feature vector of the image A. To ascertain the most effective projection vector X which encompasses the total scatter of the projection samples, the trace of the covariance matrix criterion is employed as illustrated in Eq. (2):

$$J(\boldsymbol{X}) = tr(S_x); \tag{2}$$

where, J (X) represents the trace of S_x, and S_x refers to the covariance matrix of the projected feature vectors obtained from the training images. Thus, S_x can be expressed as:

$$\begin{aligned} Sx &= E(\boldsymbol{Y} - E(\boldsymbol{Y}))E(\boldsymbol{Y} - E(\boldsymbol{Y}))^T \\ &= E(\boldsymbol{AX} - E(\boldsymbol{AX}))(\boldsymbol{AX} - E(\boldsymbol{AX}))^T \qquad (3) \\ &= E((\boldsymbol{A} - E(\boldsymbol{A}))\boldsymbol{X})((\boldsymbol{A} - E(\boldsymbol{A}))\boldsymbol{X})^T \end{aligned}$$

Hence,

$$tr(S_x) = tr(\boldsymbol{X}^T E((\boldsymbol{A} - E(\boldsymbol{A}))^T (\boldsymbol{A} - E(\boldsymbol{A})))\boldsymbol{X}) \tag{4}$$

Assuming there are M training face images, the covariance matrix, referred to as G_t can be expressed as in Eq. (5):

$$G_t = \frac{1}{M}\sum_{i=1}^{M}(\boldsymbol{A_i} - \bar{\boldsymbol{A}})^T (\boldsymbol{A_i} - \bar{\boldsymbol{A}}) \tag{5}$$

where, the A_i represents the ith training images. M denotes the number of training images and $\bar{A}$ is the average image of all training images. By calculating the eigenvectors of G_t and selecting the eigenvectors $X_1; \ldots\ldots :X_d$ corresponding to the largest eigenvalues, we obtain the optimal projection axes. Since the size of G_t is only $n \times n$, the computation of its eigenvectors proves to be more efficient than that of PCA.

The feature matrix for each image in the gallery is obtained by multiplying it by the selected eigenvectors as outlined in Eq. (8):

$$\boldsymbol{Y} = \boldsymbol{AX} \tag{6}$$

where, X is the selected eigenvector matrix and Y indicates the feature matrix corresponding to the image A. The identical equation applies to the test image. Following this, the nearest neighbour, which has a defining distance, is utilized for classification.

III. DISTANCE MEASURES

A range of distance methods have been introduced alongside the 2DPCA algorithm. In this paper, different variations of distance methods are tailored based on the structure of distance methods presented in [20]. Let $\boldsymbol{Y}_t$ is the feature matrix of a test image, $\boldsymbol{Y}_i$ is a feature matrix of a train image. The definitions of modified distance methods are as follows:

A. ***Minkowski distance (L_p metrics):*** *it is the same as AMD distance methods:*

$$d_{AMD}(\boldsymbol{Y}_t; \boldsymbol{Y}_i) = \left(\|\boldsymbol{Y}_t - \boldsymbol{Y}_i\|_2^p\right)^{1/p}$$

B. ***Manhattan distance (L_1 metrics, city block distance)***

$$d_{2MAND}(\boldsymbol{Y}_t; \boldsymbol{Y}_i) = |(\boldsymbol{Y}_t - \boldsymbol{Y}_i)|$$

C. ***Euclidean distance (L2 metrics):*** *it is the same as 2D Euclidean distance*

$$d_{2D}(\boldsymbol{Y}_t; \boldsymbol{Y}_i) = \|\boldsymbol{Y}_t - \boldsymbol{Y}_i\|_2$$

D. ***Squared Euclidean distance (sum square error, SSE), mean square error (MSE)***

$$d_{2SSED}(\boldsymbol{Y}_t; \boldsymbol{Y}_i) = \|\boldsymbol{Y}_t - \boldsymbol{Y}_i\|_2^2$$

$$d_{2MSED}(\boldsymbol{Y}_t; \boldsymbol{Y}_i) = \frac{1}{n}\|\boldsymbol{Y}_t - \boldsymbol{Y}_i\|_2^2$$

Where n is the number of selected eigenvectors.

E. ***Angle-based distance***

$$d_{2ANGD}(\boldsymbol{Y}_t; \boldsymbol{Y}_i) = \frac{\boldsymbol{Y}_t .* \boldsymbol{Y}_i}{\sqrt{\boldsymbol{Y}_t^2 .* \boldsymbol{Y}_i^2}}$$

F. ***Correlation coefficient-based distance***

$$d_{2ANGD}\,(\boldsymbol{Y}_t;\boldsymbol{Y}_i) \;=\; \frac{n * \boldsymbol{Y}_t \,.*\, \boldsymbol{Y}_i}{\sqrt{(\boldsymbol{n} * (\boldsymbol{Y}_t^2 - \boldsymbol{Y}_t{}^2).*(\boldsymbol{Y}_i^2 - \boldsymbol{Y}_i{}^2)}}$$

Where n is the number of selected eigenvectors.

G. ***Mahalanobis distance and Mahalanobis distance between normed vectors***

$$d_{2MAHD}(\boldsymbol{Y}_t;\boldsymbol{Y}_i) = z * (\boldsymbol{Y}_t - \boldsymbol{Y}_i)^T * (\boldsymbol{Y}_t - \boldsymbol{Y}_i) \qquad z = \sqrt{\frac{\boldsymbol{A}}{\boldsymbol{A} + \boldsymbol{\alpha}^2}}$$

$$d_{2MAHND}(\boldsymbol{Y}_t;\boldsymbol{Y}_i) = \frac{z.*\,(\boldsymbol{Y}_t - \boldsymbol{Y}_i)^T * (\boldsymbol{Y}_t - \boldsymbol{Y}_i)}{\sqrt{\boldsymbol{Y}_t^2}\sqrt{\boldsymbol{Y}_i^2}} \qquad z = \sqrt{\frac{1}{\boldsymbol{A}}}$$

Where A is the sorted eigenvector and $\alpha = 0.25$

H. ***Weighted Manhattan distance***

$$\boldsymbol{d}_{\boldsymbol{2WMAND}}(\boldsymbol{Y}_t;\boldsymbol{Y}_i) = z.*\,|(\boldsymbol{Y}_t - \boldsymbol{Y}_i)| \qquad z = \sqrt{\frac{1}{\boldsymbol{A}}}$$

Where A is the sorted eigenvector.

I. ***Weighted SSE distance***

$$d_{2WSSED}\,(\boldsymbol{Y}_t;\boldsymbol{Y}_i) = z.*\,\|\boldsymbol{Y}_t - \boldsymbol{Y}_i\|_2^2 \qquad z = \sqrt{\frac{1}{\boldsymbol{A}}}$$

Where A is the sorted eigenvector.

J. ***Weighted angle-based distance***

$$d_{2ANGD}\,(\boldsymbol{Y}_t;\boldsymbol{Y}_i) = \frac{z.*\,\boldsymbol{Y}_t \,.*\, \boldsymbol{Y}_i}{\sqrt{\boldsymbol{Y}_t^2 \,.*\, \boldsymbol{Y}_i^2}} \qquad z = \sqrt{\frac{1}{\boldsymbol{A}}}$$

K. ***Chi square distance***

$$d_{2CHSD}\,(\boldsymbol{Y}_t;\boldsymbol{Y}_i) = \frac{(\boldsymbol{Y}_t - \boldsymbol{Y}_i)^2}{\boldsymbol{Y}_t + \boldsymbol{Y}_i}$$

L. ***Canberra distance***

$$d_{2CNBD}\,(\boldsymbol{Y}_t;\boldsymbol{Y}_i) = \frac{|\boldsymbol{Y}_t - \boldsymbol{Y}_i|}{|\boldsymbol{Y}_t| + |\boldsymbol{Y}_i|}$$

M. ***Modified Manhattan distance***

$$d_{2MMAND}(\boldsymbol{Y}_t;\boldsymbol{Y}_i) = \frac{|(\boldsymbol{Y}_t - \boldsymbol{Y}_i)|}{|\boldsymbol{Y}_t|.*\,|\boldsymbol{Y}_i|}$$

N. ***Modified SSE-based distance***

$$d_{2MSSED}\,(\boldsymbol{Y}_t;\boldsymbol{Y}_i) = \frac{\|\boldsymbol{Y}_t - \boldsymbol{Y}_i\|_2^2}{\|\boldsymbol{Y}_t\|_2^2.*\,\|\boldsymbol{Y}_i\|_2^2}$$

O. ***Weighted modified Manhattan distance***

$$d_{2WMMAND}(\boldsymbol{Y}_t;\boldsymbol{Y}_i) = \frac{z.*\,|(\boldsymbol{Y}_t - \boldsymbol{Y}_i)|}{|\boldsymbol{Y}_t|.*\,|\boldsymbol{Y}_i|} \qquad z = \sqrt{\frac{1}{\boldsymbol{A}}}$$

P. ***Weighted modified SSE-based distance***

$$d_{2WMSSED}\,(\boldsymbol{Y}_t;\boldsymbol{Y}_i) = \frac{z.*\,\|\boldsymbol{Y}_t - \boldsymbol{Y}_i\|_2^2}{\|\boldsymbol{Y}_t\|_2^2.*\,\|\boldsymbol{Y}_i\|_2^2} \qquad z = \sqrt{\frac{1}{\boldsymbol{A}}}$$

IV. EXPERIMENTS AND DISCUSSION

A. Result tested on ORL database

The ORL database [37] contains 400 images for 40 individuals, with 10 different images for each one. The image measures 112×92. The images were captured against a dark homogeneous background at different times, with facial expressions (open/closed eyes, smiling / not smiling), lighting variations, and facial details (glasses / no glasses), while allowing for some lateral movement. Some examples of ORL are shown in Fig. 1.

Fig. 1: Examples from the ORL database used in the experiments

To evaluate the different distance methods on the ORL database, the first 1 to 9 images are selected for training, and the remaining images are used for testing. It is evaluated with a different number of eigenvectors. Table 1 shows the best accuracy with the corresponding number of eigenvectors.

Table 1: Best accuracy of ORL database with the corresponding number of eigenvectors for modified distance methods

N0 of training Images	Manhattan		Squared Euclidean (SSE)		Mean square Euclidean (MSE)		Angle-based		Correlation coefficient-based		Weighted Manhattan		Mahalanobis Norm		Weighted SSE		Weighted angle-based		Chi square		Canberra		Modified Manhattan distance		Modified SSE-based		Weighted modified Manhattan		Weighted modified SSE-based		2D Euclidean	
	accuracy	No. eigenVectors	accuracy	No. eigenVectors	accuracy	No. eigenVectors	accuracy	No. eigenVectors	accuracy	No. eigenVectors	accuracy	No. eigenVectors	accuracy	No. eigenVectors	accuracy	No. eigenVectors	accuracy	No. eigenVectors	accuracy	No. eigenVectors	accuracy	No. eigenVectors	accuracy	No. eigenVectors	accuracy	No. eigenVectors	accuracy	No. eigenVectors	accuracy	No. eigenVectors	accuracy	No. eigenVectors
1	75.56	3	73.06	2	73.06	2	68.89	5	63.89	6	74.17	2	65.56	5	74.44	2	65.56	5	68.06	2	71.39	2	73.61	2	70.56	4	63.61	2	70.83	2	75.56	6
2	85.94	4	84.06	2	84.06	2	78.13	6	75.63	12	85.63	4	74.69	5	85.94	2	74.69	5	78.13	2	78.75	2	83.13	4	80.63	4	72.19	2	79.69	2	85.94	2
3	88.21	6	85.71	14	85.71	14	79.29	4	79.64	6	87.86	4	78.21	8	86.43	4	78.21	8	83.57	2	83.21	2	82.86	2	81.43	2	77.50	2	82.14	2	87.86	6
4	91.25	11	89.17	8	89.17	8	83.33	5	82.08	6	90.00	4	83.33	9	89.58	4	83.33	9	80.42	2	86.25	2	87.50	5	85.00	4	80.83	2	83.33	2	90.83	12
5	93.50	9	91.50	8	91.50	8	86.50	4	84.00	9	93.00	4	82.00	9	91.00	4	82.00	9	80.50	1	86.00	5	91.00	3	88.50	4	85.00	2	86.50	4	93.50	15
6	96.88	3	96.88	6	96.88	6	93.13	4	90.00	7	96.25	3	88.13	7	96.88	5	88.13	7	89.38	1	91.88	2	97.50	3	95.00	3	93.13	2	96.25	3	97.50	7
7	96.67	2	96.67	6	96.67	6	93.33	4	91.67	7	96.67	2	90.83	8	96.67	5	90.83	8	89.17	1	94.17	5	99.17	3	95.83	3	90.83	2	97.50	3	97.50	3
8	96.25	2	96.25	5	96.25	5	96.25	4	93.75	7	97.50	3	95.00	9	96.25	5	95.00	9	87.50	1	96.25	5	98.75	3	96.25	3	92.50	2	97.50	3	97.50	3
9	95.00	3	95.00	6	95.00	6	100.00	4	97.50	7	97.50	3	95.00	6	95.00	3	95.00	6	87.50	2	95.00	2	97.50	3	95.00	3	95.00	2	97.50	3	95.00	3

It can be seen from Table 1 that the angle-based method achieves the best accuracy when the number of training images is 9, which is 100%. In contrast, for the other sets of training images, both Manhattan and modified Manhattan demonstrate superior results compared to other distance methods. Figure 2 displays the average accuracy outlined in Table 1.

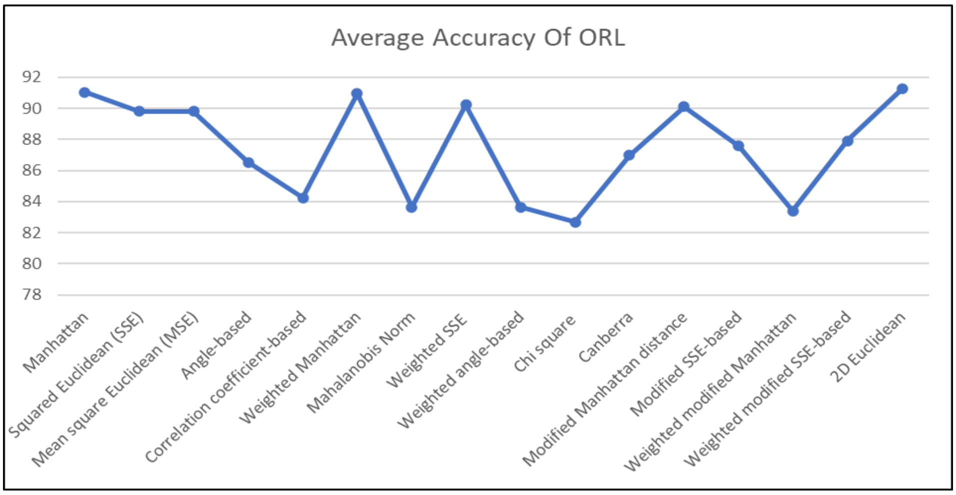

Fig. 2: Average Accuracy of the ORL database

It is evident from Fig. 2 that Manhattan and 2D Euclidean distance methods yield the best average accuracies. In terms of the number of eigenvectors utilized, the chi-square distance method requires the fewest eigenvectors; nevertheless, it results in the lowest average accuracy. On the other hand, Weighted Manhattan and Weighted SSE utilize the least number of eigenvectors while still achieving satisfactory average accuracies.

B. Results on AR database

The AR face database [38] contains 2,600 warped frontal color images of 100 persons. Each subject has 26 different images registered in two separate sessions; each held in a different week. Each session consists of 13 images featuring various expressions and conditions: neutral expression, smile, anger, scream, left light on, right light on, all side lights on, wearing sunglasses, wearing sunglasses with left light on, wearing sunglasses with right light on, wearing a scarf, wearing a scarf with left light on, and wearing a scarf with right light on. The images were captured under controlled conditions of illumination and viewpoint using the same camera. All images were converted to grayscale and have a size of 165×120 pixels. Examples from the AR database are shown in Fig. 3.

(a) Session 1 (b) Session 2

Fig. 3. Examples of one subject in the AR face database

Natural images of the two sessions are used for training, and the rest of the expressions and conditions are used for testing individually for both sessions. Table 2 shows the best accuracy and the corresponding number of eigenvectors for each state individually for both sessions.

Table 2: Best accuracy of AR database with the corresponding number of eigenvectors for modified distance methods

N0 of training Images	Manhattan		Squared Euclidean		Mean square Euclidean		Angle-based		Correlation coefficient-		Weighted Manhattan		Mahalanobis Norm		Weighted SSE	
	accuracy	No. eigenVectors	accuracy	No. eigenVectors	accuracy	No. eigenVectors	accuracy	No. eigenVectors	accuracy	No. eigenVectors	accuracy	No. eigenVectors	accuracy	No. eigenVectors	accuracy	No. eigenVectors
smile	94.00	14	97.50	20	97.50	20	95.50	18	96.00	15	99.00	9	94.00	14	98.00	10
anger	85.50	18	90.50	9	90.50	9	86.50	18	87.50	20	93.50	9	85.50	18	92.50	7
scream	45.50	6	61.50	6	61.50	6	49.00	16	49.00	11	77.50	6	45.50	6	64.50	8
left light on	90.00	4	19.00	20	19.00	20	90.00	4	93.50	4	82.50	20	90.00	4	51.00	20
right light on	76.50	20	15.50	18	15.50	18	67.00	20	94.50	15	56.00	20	76.50	20	36.50	20
all side lights on	87.50	18	2.50	7	2.50	7	87.50	19	93.50	18	59.00	20	87.50	18	14.50	20
wearing sunglasses	73.00	18	42.50	14	42.50	14	76.00	19	78.50	19	90.50	7	73.00	18	67.00	20
sunglasses with left light on	51.50	20	37.50	17	37.50	17	54.50	20	67.00	20	64.50	20	51.50	20	53.50	20
sunglasses with right light on	33.50	19	25.50	20	25.50	20	30.50	19	61.50	19	34.50	11	33.50	19	35.50	20
wearing a scarf	73.00	20	9.50	14	9.50	14	74.00	20	75.50	20	51.50	9	73.00	20	12.00	15
scarf with left light on	55.00	20	13.00	15	13.00	15	57.00	20	62.50	20	36.00	20	55.00	20	24.00	19
scarf with right light on	34.00	20	13.00	10	13.00	10	23.00	3	55.00	20	12.50	4	34.00	20	12.50	4

N0 of training Images	Weighted angle-based		Chi square		Canberra		Modified Manhattan		Modified SSE-based		Weighted modified		Weighted modified SSE-		2D Euclidean	
	accuracy	No. eigenVectors	accuracy	No. eigenVectors	accuracy	No. eigenVectors	accuracy	No. eigenVectors	accuracy	No. eigenVectors	accuracy	No. eigenVectors	accuracy	No. eigenVectors	accuracy	No. eigenVectors
smile	98.00	10	91.00	1	99.50	15	94.50	2	89.50	1	92.00	2	89.50	1	98.00	12
anger	92.50	7	74.00	1	96.50	11	88.00	3	78.50	13	81.50	2	77.00	13	91.50	12
scream	64.50	8	33.50	1	84.00	17	51.00	2	42.50	2	45.50	2	42.00	2	63.50	6
left light on	51.00	20	22.00	14	81.00	20	82.50	4	84.00	4	32.50	4	83.00	4	53.50	19
right light on	36.50	20	9.50	15	51.00	20	36.00	3	54.50	3	20.50	3	54.00	3	38.50	20
all side lights on	14.50	20	9.50	10	68.00	20	42.50	14	33.50	13	8.50	8	29.00	9	22.50	20
wearing sunglasses	67.00	20	26.50	16	95.00	12	79.50	2	40.00	15	73.50	2	39.50	2	67.00	15
sunglasses with left light on	53.50	20	16.50	2	65.00	19	24.50	4	13.50	4	5.50	4	13.50	4	55.00	20
sunglasses with right light on	35.50	20	13.00	2	41.00	20	11.50	13	7.00	11	3.50	8	7.00	11	41.00	19
wearing a scarf	12.00	15	10.50	18	90.50	16	80.00	14	60.50	15	23.00	2	57.00	13	17.50	20
scarf with left light on	24.00	19	8.50	20	51.50	20	42.00	4	32.00	4	10.00	4	33.00	4	33.00	19
scarf with right light on	12.50	4	4.50	3	16.00	20	21.50	3	17.50	3	6.50	2	17.00	3	17.50	12

From Table 2, it can be observed that Canberra provides the best accuracy result of 99.5% when the image is normal and the person is smiling. Nevertheless, the Correlation coefficient-based approach achieves better accuracies in most cases. The Chi-square method remains unchanged, as observed in the ORL database, which produces the lowest accuracies. Figure 4 illustrates the average accuracy outlined in Table 2.

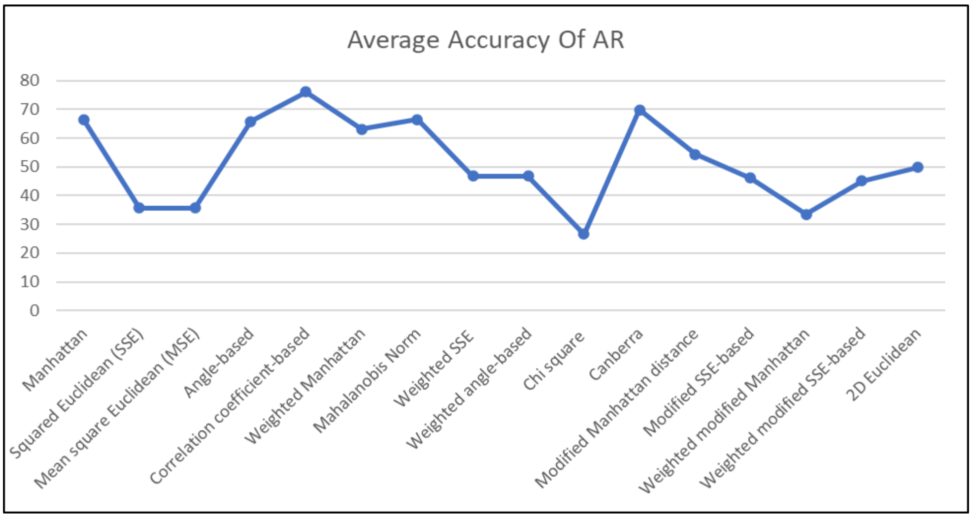

Fig. 4: Average Accuracy of the AR database

It is apparent from Fig. 4 that the Correlation coefficient-based and Canberra methods yield the best average accuracies. Regarding the number of selected eigenvectors, the Weighted modified Manhattan distance method requires the fewest eigenvectors; nonetheless, it results in a low average accuracy. Conversely, the Correlation coefficient utilizes more than the average number of eigenvectors while achieving the best average accuracy.

V. Results on LFW database

Labeled Faces in the Wild (LFW) [39] was developed by the University of Massachusetts, Amherst. It contains 13,233 images of 5,749 individuals, featuring significant variations in pose, occlusion, illumination, and expression. The database comprises images of famous people from the internet, aimed at studying the face recognition problem in unconstrained environments. Among the individuals, 1,680 have two or more distinct images, while the remaining individuals have only one image. The images are in JPEG format, each measuring 250×250 pixels. While some images are grayscale, the majority are in color. A sub-database is derived from this dataset, selecting individuals with 10 or more images, from which 10 images are chosen. Consequently, the new database consists of 100 individuals, each with 10 images. These images are cropped, resized to 80×60 pixels, and aligned using the method described in [40]. Examples from the LFW face database are shown in Fig. 5.

Fig. 5. Examples of three subjects in the LFW database

To evaluate the different distance methods on the LFW database, the first 1 to 9 images are selected for training, and the rest are for testing. It is evaluated with a different number of eigenvectors. Table 3 shows the best accuracy with the corresponding number of eigenvectors.

Table 3: Best accuracy of AR database with the corresponding number of eigenvectors for modified distance methods

N0 of training Images	Manhattan		Squared Euclidean (SSE)		Mean square Euclidean (MSE)		Angle-based		Correlation coefficient-based		Weighted Manhattan		Mahalanobis Norm		Weighted SSE		Weighted angle-based		Chi square		Canberra		Modified Manhattan distance		Modified SSE-based		Weighted modified Manhattan		Weighted modified SSE-based		2D Euclidean	
	accuracy	No. eigenVectors	accuracy	No. eigenVectors	accuracy	No. eigenVectors	accuracy	No. eigenVectors	accuracy	No. eigenVectors	accuracy	No. eigenVectors	accuracy	No. eigenVectors	accuracy	No. eigenVectors	accuracy	No. eigenVectors	accuracy	No. eigenVectors	accuracy	No. eigenVectors	accuracy	No. eigenVectors	accuracy	No. eigenVectors	accuracy	No. eigenVectors	accuracy	No. eigenVectors	accuracy	No. eigenVectors
1	16.67	17	18.67	8	18.67	8	25.44	1	33.11	6	20.22	12	25.44	1	19.78	13	25.44	1	14.11	1	20.11	10	16.67	8	14.33	1	13.11	1	14.33	1	20.44	8
2	25.25	12	26.88	15	26.88	15	33.13	9	42.00	11	28.13	9	31.13	9	27.38	17	31.13	9	18.88	1	30.13	18	25.25	9	20.63	4	17.13	1	20.75	4	28.88	17
3	30.71	9	33.00	15	33.00	15	41.57	11	52.14	9	34.14	8	40.00	9	33.43	9	40.00	9	22.00	1	37.14	15	30.71	11	27.57	9	22.00	1	25.86	9	34.71	9
4	37.17	9	40.83	11	40.83	11	48.00	11	59.17	9	41.50	9	47.00	9	40.17	9	47.00	9	28.17	1	43.50	15	37.17	9	33.17	9	26.33	1	31.17	4	43.00	9
5	40.80	10	44.00	16	44.00	16	52.00	11	61.80	9	45.60	8	49.40	6	44.40	17	49.40	6	30.00	1	49.80	14	40.80	9	35.80	9	28.40	1	35.20	4	46.40	9
6	44.50	15	44.50	16	44.50	16	55.25	10	63.25	9	50.50	9	53.00	9	49.50	18	53.00	9	34.50	1	52.75	18	44.50	9	39.00	9	30.50	1	37.25	4	49.00	14
7	46.67	15	52.67	16	52.67	16	59.33	10	67.33	9	55.33	9	57.67	9	55.67	13	57.67	9	36.67	1	56.67	18	46.67	10	44.00	4	34.00	1	46.33	4	56.67	12
8	47.50	15	54.00	10	54.00	10	63.00	10	70.00	7	55.50	9	59.50	9	57.00	14	59.50	9	39.00	1	60.00	15	47.50	6	45.50	7	36.50	1	45.00	4	57.50	17
9	50.00	6	58.00	6	58.00	6	67.00	10	70.00	7	59.00	9	61.00	8	61.00	11	61.00	8	43.00	1	59.00	13	50.00	5	46.00	4	41.00	1	46.00	7	62.00	9

From Table 3, one can observe that the method utilizing the Correlation coefficient-based method delivers the best accuracy result of 70%. Furthermore, it also achieves the best accuracy in all cases. In contrast, the Weighted modified Manhattan produces the lowest accuracies in nearly all cases. Figure 6 depicts the average accuracy presented in Table 3.

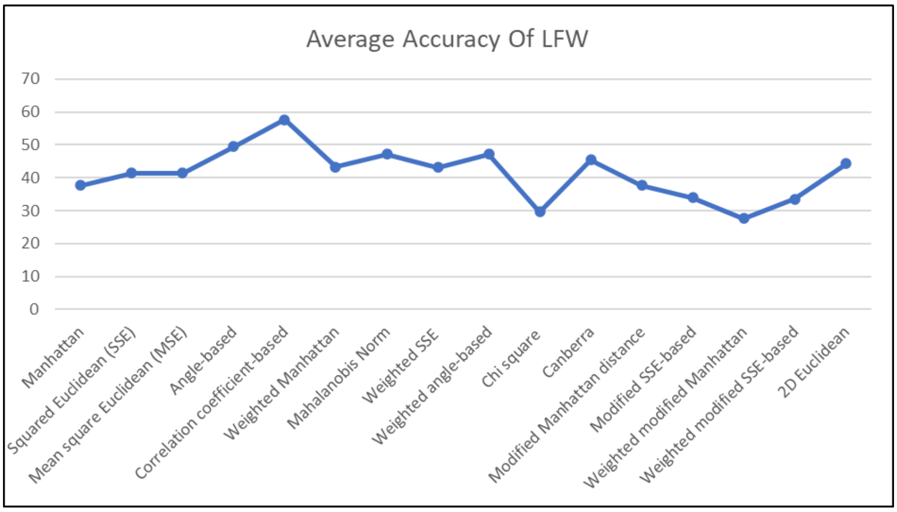

Fig. 6: Average Accuracy of the LFW database

It is clear from Fig. 6 and Table 3 that the Correlation coefficient-based and Angle-based methods deliver the best accuracies. With respect to the number of selected eigenvectors, the Weighted modified Manhattan distance and Chi square methods use the fewest eigenvectors; still, they yield a low average accuracy. On the other hand, the Correlation coefficient utilizes fewer than the average number of eigenvectors and concurrently achieves the best average accuracy.

Based on the analysis of the three databases, it can be inferred that the Correlation Coefficient-based method is superior to other distance methods, particularly regarding accuracy and the number of eigenvectors. Furthermore, it is apparent that both Angle-based and Canberra methods are noteworthy distance methods and require additional research in diverse situations.

VI. CONCLUSIONS AND FUTURE WORK

The efficiency of 14 distance methods applied with Two-Dimensional Principal Component Analysis (2DPCA) in face recognition is examined. Different experiments on three well-known databases are conducted. These experiments show the superiority of the correlation coefficient-based method, which achieves the highest accuracy. This demonstrates its effectiveness under different variations of face conditions. Furthermore, the considerable accuracies of both the angle-based and Canberra distance methods reveal their effectiveness in specific variations.

Several tracks need to be explored to reveal the impacts of the different distance methods. Initially, the effect of existing specific different pose variations is a particular issue. Furthermore, what is the impact of the preprocess algorithms with different distance methods? The influence of distance metrics in real-time face recognition systems is a crucial issue in practical deployment regarding security and surveillance. Furthermore, 2DPCA should be explored with advanced machine learning approaches, including deep learning, which may increase the reliability and accuracy of recognition systems.

REFERENCES

[1] .S. Z. Li and A. K. Jain, Handbook of Face Recognition, Springer, 2005.
[2] .K. Kim et al., “Face recognition using kernel principal component analysis,” IEEE Signal Process. Lett., vol. 9, no. 2, pp. 40–42, 2002.
[3] .H. Moon and P. J. Phillips, “Computational and performance aspects of PCA-based face-recognition algorithms,” Perception, vol. 30, no. 3, pp. 303–321, 2001.
[4] .R. Tjahyadi et al., “Automatic parameter selection for Eigenfaces,” in Proc. ICOTA, 2004.
[5] .H. Meng and X. Ke, “Further research on principal component analysis method of face recognition,” in Proc. ICMA, 2008, pp. 421–425.
[6] .E. Kokiopoulou and Y. Saad, “PCA without eigenvalue calculations: a case study on face recognition,” in SIAM Data Mining Conf., 2005.
[7] .S. Gupta et al., “A new optimized approach to face recognition using Eigenfaces,” Global J. Computing Sci. Technol., 2010.
[8] .L. Wiskott et al., “Face recognition by elastic bunch graph matching,” IEEE Trans. PAMI, vol. 19, no. 7, pp. 775–779, 1997.
[9] .J. Yang et al., “Two-dimensional PCA: a new approach to appearance-based face representation and recognition,” IEEE Trans. PAMI, vol. 26, no. 1, pp. 131–137, 2004.
[10] .D. Zhang and Z. Zhou, “Diagonal principal component analysis for face recognition,” Pattern Recognition, vol. 39, no. 1, pp. 140–142, 2006.
[11] .A. L. Koerich et al., “Face recognition using selected 2DPCA coefficients,” in Proc. IWSSIP, 2010.
[12] .Y. Zeng et al., “Face recognition based on the variation of 2DPCA,” J. Computing Inf. Syst., vol. 7, no. 1, pp. 303–310, 2011.
[13] .B. A. Draper et al., “Recognizing faces with PCA and ICA,” CVIU, vol. 91, no. 1–2, pp. 115–137, 2003.

[14] .C. D. Meyer, Matrix Analysis and Applied Linear Algebra, SIAM, 2000.
[15] .W. Liwei et al., “On the Euclidean distance of images,” IEEE Trans. PAMI, vol. 27, no. 8, pp. 1334–1339, 2005.
[16] .W. Zuo et al., “An assembled matrix distance metric for 2DPCA-based recognition,” Pattern Recognition Lett., 2006.
[17] .J. Meng and W. Zhang, “Volume measure in 2DPCA-based face recognition,” Pattern Recognition Letters, 2007.
[18] .Z. Xu et al., “Boosting for learning a similarity measure in 2DPCA,” in Proc. IEEE CSIE, 2009.
[19] .W. H. Al-Arashi and S. A. Suandi, “2DPCA-based Row-kNN distance computation for face recognition,” in Proc. SPIE ICDIP, 2012.
[20] .V. Perlibakas, “Distance measures for PCA-based face recognition,” Pattern Recognition Letters, 2004.
[21] .P. Huang et al., “F-norm distance metric based robust 2DPCA and face recognition,” Neural Computing Appl., 2023.
[22] .B. Zhao et al., “Relaxed two-dimensional PCA for robust face recognition,” Neural Networks, 2020.
[23] .W. Zhao et al., “Face recognition: a literature survey,” ACM Computing Survey, vol. 35, no. 4, pp. 399–458, 2003.
[24] .F. Alsaqre, “An improved fractional two-dimensional principal component analysis for face recognition,” Jordanian Journal of Computers and Information Technology, vol. 8, no. 1, pp. 1–11, 2022.
[25] .A. Maafiri, Y. Ruichek, L. A. Hussein, and S. A. Al-Mahmoud, “Lwkpca: A new robust method for face recognition under adverse conditions,” IEEE Access, vol. 10, pp. 60192–60204, 2022.
[26] .A. Hafiane, G. Seetharaman, and B. Zavidovique, "Median Gabor 2DPCA for texture classification," IEEE Trans. Image Process., vol. 24, no. 12, pp. 5374–5388, 2015.
[27] .H. Shan, Y. Li, J. Bi, and T. Liu, "Two-dimensional PCA for medical image feature extraction and disease classification," IEEE Access, vol. 9, pp. 102345–102356, 2021.
[28] .H. Li, W. Li, Q. Du, and L. Zhang, "A 2DPCA-based feature extraction method for hyperspectral image classification," IEEE J. Sel. Top. Appl. Earth Obs. Remote Sens., vol. 11, no. 5, pp. 1408–1420, 2018.
[29] .N. Sharma, U. Pal, F. Kimura, and S. Pal, "Recognition of offline handwritten Devanagari characters using quadratic classifier and 2DPCA," Pattern Recognition Lett., vol. 30, no. 5, pp. 430–436, 2009.
[30] .Z. Zhang, Y. Chen, and C. Li, "Hybrid deep learning and 2DPCA-based texture classification for smart manufacturing," IEEE Access, vol. 9, pp. 118956–118967, 2021.
[31] .D. Wang, J. Zhang, and X. Liu, "Two-dimensional PCA and CNN hybrid network for early lung cancer detection," Computers in Biology and Medicine, vol. 137, 104795, 2021.
[32] .L. Fang, Y. Li, and B. Wang, "Spectral–spatial feature extraction using 2DPCA and 3D-CNN for hyperspectral image classification," Remote Sensing, vol. 12, no. 3, p. 456, 2020.
[33] .F. Li, Z. Huang, and X. Xiao, "Handwritten character recognition combining 2DPCA features and convolutional recurrent neural networks," Pattern Recogn. Lett., vol. 139, pp. 151–158, 2020.
[34] .W. Ge, J. Li, X. Wang, and T. Zielinska, "Robust two-dimensional PCANet with F-norm distance metric," Knowledge-Based Systems, vol. 295, p. 111777, July 2024.
[35] .Z. Tan and H. Yang, "Reweighted angle two-dimensional principal component analysis for feature extraction," Pattern Recognition, vol. 168, pp. 111817, December 2025.
[36] .Al-Arashi, W. H., Shing, C. W., and Suandi, S. A., "RowAMD Distance: A Novel 2DPCA-Based Distance Computation with Texture-Based Technique for Face Recognition," Transactions on Internet and Information Systems (TIIS), vol. 11, pp. 5474-5490, 2017.
[37] .ORL, “The ORL face database at the AT&T (Olivetti) Research Laboratory.” Available from: http://www.uk.research.att.com/facedatabase.html (1992).
[38] .Martínez, A. M. and Kak, A. C., “PCA Versus LDA,” IEEE Transactions on Pattern Analysis and Machine Intelligence, vol. 23, pp. 228–233, 2001.
[39] .Huang, G. B., Mattar, M., Berg, T. and Learned-Miller, E., “Labeled Faces in The Wild: A Database for Studying Face Recognition in Unconstrained Environments,” Technical report, University of Massachusetts, Amherst, pp. 07-49, 2007.
[40] .Peng, Y., Ganesh, A., Wright, J., Xu,W. and Ma, Y., “RASL: Robust Alignment by Sparse and Low-Rank Decomposition for Linearly Correlated Images,” IEEE Transactions on Pattern Analysis and Machine Intelligence, vol. 34, pp. 2233–2246, 2012.
[41]